Numerical Methods in Civil Engineering

Controlling structures by inverse adaptive neuro fuzzy inference system and MR dampers

M. Rezaiee-Pajand*, A. Baghban**

Abstract:

To control structures against wind and earthquake excitations, Adaptive Neuro Fuzzy Inference Systems and Neural Networks are combined in this study. The control scheme consists of an ANFIS inverse model of the structure to assess the control force. Considering existing ANFIS controllers, which require a second controller to generate training data, the authors' approach does not need another controller. To generate control force, active and semi-active devices could be used. Since the active ANFIS inverse controller may not guarantee a satisfactory response due to different uncertainties associated with operating conditions and noisy training data, this paper uses MR dampers as semi-active devices to provide control forces. To overcome the difficulty of tuning command voltage of MR dampers, a neural network inverse model is developed. The effectiveness of the proposed strategy is verified and illustrated using simulated response of the 3-story full-scale nonlinear benchmark building excited by several earthquake records through computer simulation. Moreover, the recommended control algorithm is validated using the wind-excited 76-story benchmark building equipped with MR and TMD dampers. Comparing results with other controllers demonstrates that the proposed method can reduce displacement, drift and acceleration, significantly.

1. Introduction

With the increasing studies in the field of structural control, various control methods have been proposed. Generally, these schemes can be divided into two groups. The first one comprises control strategies that require accurate mathematical formulation for the structural model. Although structural models can be developed, there are many sources of uncertainty, measurement noise and nonlinearity that reduce effectiveness of control algorithms. LQR, LQG, H2 and sliding model control techniques are

some instances of this group. In recent years, there has been a growing trend toward utilization of intelligent control as a second group of control methods (Al-Dawod *et al.* 2004[1]; Pourzeynali *et al.* 2007[20]; Rezaiee-Pajand *et al.* 2009[21]; Karamodin *et al.* 2012[10]; Marinaki *et al.* 2015[16]; Park & Ok 2015[19]). This group of controllers which does not require an accurate mathematical model of structure includes neural network and fuzzy control methods.

Fuzzy logic provides a Powerful tool for utilization of human expert knowledge in complement to mathematical knowledge. The main advantages of the fuzzy controller are:

(a) It is capable of handling the non-linear behavior of the structures.

* Corresponding Author: Professor, Civil Engineering Department, Ferdowsi University of Mashhad, Iran. Email: rezaiee@um.ac.ir.

** PhD student., Civil Engineering Department, Ferdowsi University of Mashhad, Iran. Email:Baghban.k@gmail.com.

(b) It can tolerate uncertainties such as structural uncertainties and assumed loading distribution.

(c) It is one of the few mathematical model-free approaches for structural control.

(d) It can be adapted to new situations by modifying its rules or membership functions.

Artificial Neural Network (ANN) controller is another control method, which is associated with intelligent control methods. ANN is a system that includes a number of similar non-linear processing elements. These processing elements operate in parallel and are arranged in patterns similar to the patterns found in biological neural nets. The processing elements or nodes are connected to each other by adjustable weights. These weights will change in such a way to achieve a desired input-output relationship. ANNs can be used for time series prediction, classification, and control and identification purposes. Several strategies have been presented for structural control using ANNs (Jung *et al.* 2004[8]; Bani-Hani *et al.* 2006[2]; Lee *et al.* 2006[15]; Kumar *et al.* 2007[12]).

Adaptive-network-based fuzzy inference system (ANFIS) is a very powerful approach for modeling complex and nonlinear systems (Kadhim 2011[9]). It has the advantages of learning capability of neural networks and expert knowledge of fuzzy logic. ANFIS includes a fuzzy inference system whose membership functions are interactively adjusted according to a given set of input and output data. Schurter & Roschke (2001)[22] and Gu & Oyadiji (2008)[6] used ANFIS for control of structure. In their approach, training data was generated using LQR and LQG controllers, respectively. The disadvantage of training ANFIS using other controllers is that, the trained ANFIS controller works worse than the reference controllers, in most situations. In best conditions, an ANFIS controller can work as well as reference controllers.

Since the semi-active control combines the adaptability associated with active control and the reliability associated with passive control, it is generating great interest among researchers in the field of structural control (Choi *et al.* 2004[3]; K-Karamodin *et al.* 2008[14]; Karamodin *et al.* 2012[10]; Kerboua *et al.* 2014[11]). The magnetorheological (MR) damper is a device in this class that generates force in response to velocity and applied voltage. Because of the inherent nonlinear nature of this device, one of the challenging aspects of utilizing this technology is in the development of suitable control algorithms. Several strategies have been developed for control of MR dampers. Dyke *et al.* (1996)[4] developed a semi-active clipped-optimal control algorithm to reduce the response of structure with a MR damper. In their strategy, the command voltage of the MR damper was tuned by a linear optimal controller combined with a force feedback loop. The command signal was adjusted at either zero or the

maximum level, depending on how the damper's force compared with the desired optimal control force. Choi *et al.* (2004)[3] presented a semi-active fuzzy control strategy for seismic response reduction using an MR damper. In their approach, the output variable of the fuzzy controller was the command voltage of MR damper. Karamodin *et al.* (2008)[14] designed a neuro-predictive algorithm to predict the voltage command of MR damper to provide the control force determined by LQG controller.

In this paper, ANFIS based inverse model control is developed for semi-active control of structures based on acceleration feedback. This method is a straightforward method to design a controller in which the controller is the inverse of the plant. This approach only needs one learning task to find the plant inverse and doesn't require other controllers to generate training data. Here, MR dampers are selected as semi-active devices to provide control forces. To set the command voltage of each MR damper in order to provide the desired force determined by ANFIS controller, an NN inverse model of MR damper is employed. The effectiveness of proposed strategy is verified and illustrated using simulated response of the 3-, and 76-story benchmark buildings excited by various earthquake records and wind, respectively. The results are compared with passive and active control systems.

2. Benchmark Building Model

2. 1. 3-Story Benchmark Building

The nonlinear benchmark 3-story building used for this study was defined by Ohtori et al. (2004)[17] in the problem definition paper. The building is 11.89 m in height and 36.58 m by 54.87 m in the plan. The first three natural frequencies of the 3-story benchmark evaluation model are: 0.99, 3.06, and 5.83 Hz. Four historical ground motion earthquake records (two far-field and two near-field) are selected for study: El Centro (1940), Hachinohe (1968), Northridge (1994) and Kobe (1995). Control actuators are located on each floor of the structure to provide forces to adjacent floors. Since the MR dampers capacity is limited to a maximum force of 1,000 kN, three, two and two dampers are used at the first, second and the third floors of the structure respectively to provide the required larger forces. Three sensors for acceleration measurements are employed for feedback in the control system on the first, second and third floors. Moreover, three sensors for velocity measurement are used on the floors to determine the voltage of MR dampers based on the command force.

During large seismic events, structural members can yield, resulting in nonlinear response, behavior that may be significantly different from a linear approximation. To represent the nonlinear behavior, a bilinear hysteresis model

is used to model the plastic hinges (Fig. 1). These plastic hinges, which are assumed to occur at the moment resisting column-beam and column-column connections, introduce a material nonlinear behavior of these structures.

To determine the time-domain response of such nonlinear structures, the Newmark-β Time-step integration method developed in MATLAB by Ohtori & Spencer (1999) [18] is used. The incremental equations of motion for the nonlinear structural system take the following form:

$$M\Delta\ddot{U} + C\Delta\dot{U} + K\Delta U = -MG\Delta\ddot{X}g + P\Delta f + \Delta F_{err} \quad (1)$$

where, M, C, and K are the mass, damping and stiffness matrices of the building, ΔU is the incremental response vector, G is a loading vector for the ground acceleration, $\Delta\ddot{X}g$ is the ground acceleration increment, P is a loading vector for the ground forces, Δf is the incremental control force and Δf_{err} is the vector of the unbalanced forces.
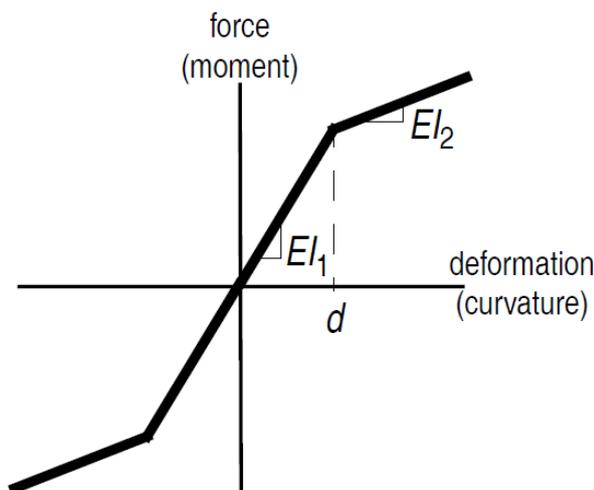

Fig. 1: Bilinear hysteresis model for structural member bending.

2. 2. 76- Story Benchmark Building

The nonlinear benchmark 76-story building used for this study was defined by Yang *et al.* (1999)[24] in the problem definition paper. The building is a 76-story 306 meters concrete office tower proposed for the city of Melbourne, Australia. It is slender with a height to the width ratio of 7.3; hence, this structure is wind sensitive. The first five natural frequencies are 0.16, 0.765, 1.992, 3.790 and 6.395 Hz, respectively. Damping ratios for the first five modes are assumed to be 1% of critical for the proportional damping matrix. A semi-active tuned mass damper (TMD) includes a MR damper and an inertial mass of 500 tons that is installed on the top floor. The mass is about 45% of the top-floor mass, which is 0.327% of the total mass of the building. The damper natural frequency is tuned to 0.16 Hz and its damping ratio is set at 20%. The well-known Davenport wind load spectrum, which has been used in the Canadian

design code, is used herein for along-wind loads. A sensor for acceleration measurement is employed for feedback in the control system on the 76th floor, and two sensors are employed for velocity measurement on the 76th floor and TMD to determine the voltage of MR damper based on the control force.

3. MR Damper Model

An MR damper typically comprises of a hydraulic cylinder, magnetic coils, and MR fluids that consist of micrometer-sized magnetically polarizable particles floating within oil-type fluids. In the presence of a magnetic field, the particles polarize and provide an increased resistance to flow. By altering the magnetic field, the desired behavior of MR dampers can be earned. Since MR fluid can be changed from a viscous fluid to a yielding solid within milliseconds, and the resulting damping force can be notably large with a low-power requirement, MR dampers are appropriate for full-scale applications (Xu *et al.* 2000[23]).

Suitable modeling of the control devices is essential for precise prediction of the behavior of the controlled system. The simple mechanical model shown in Figure 2 was developed and shown to accurately predict the behavior of the MR damper over a wide range of inputs (Dyke & Carlson 1999[5]). The equations governing the force, f, predicted by this model are as follows:

$$f = c_0\dot{x} + \alpha z \quad (2)$$
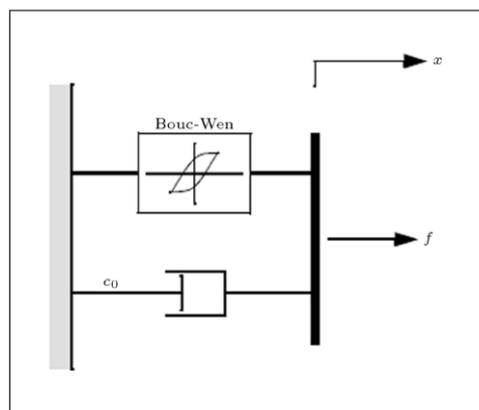$$\dot{z} = -\gamma|\dot{x}|z|z|^{n-1} - \beta\dot{x}|z|^n + A\dot{x} \quad (3)$$

Fig. 2: Mechanical model of MR damper.

Where x is the displacement of the device, and z is the evolutionary variable that accounts for the history dependence of the response. The model parameters depend on the voltage, v, to the current driver as follows:

$$\alpha = \alpha_a + \alpha_b u \quad (4a)$$
$$c_0 = c_{0a} + c_{0b} u \quad (4b)$$

where u is given as the output of the first-order filter:

$$\dot{u} = -\eta(u - v) \qquad (5)$$

Equation 5 is used to model the dynamics involved in reaching theological equilibrium and in driving the electromagnet in the MR damper (Dyke & Carlson 1999[5]). This MR damper model is used in this study to model the behavior of the MR damper. Selected parameters of the MR damper are given in Table 1:

Table 1: MR damper parameters.

| MR damper parameters			
α_a	1.0872e5 N/cm	A	1.2
α_b	4.9616e5 N/(cm V)	γ	3 cm^{-1}
c_{0a}	4.40 N s/cm	β	3 cm^{-1}
c_{0b}	44.0 N s/(cm V)	η	50 s^{-1}
n	1		

These parameters are based on the identified model of an MR damper tested at Washington University (Yi *et al.* 2001[25] & 2009[26]) and scaled up to have maximum capacity of 1000 kN with maximum command voltage Vmax= 10 V.

4. Overview of the ANFIS

ANFIS is a fuzzy Sugeno model with a framework to facilitate learning and adaptation procedure. Such framework makes fuzzy logic more systematic and less relying on expert knowledge. The objective of ANFIS is to tune the parameters of a fuzzy system by utilizing a learning procedure using input-output training data. A technique consisting of the least square algorithm and back propagation is usually used for training fuzzy inference system (Kadhim 2011[9]). Basic architecture of ANFIS which has two inputs *x* and *y* and one output *f* is shown in Figure 3. Assuming that the rule base contains two Takagi-Sugeno if-then rules as follows:

Rule 1: *If x is A₁ and y is B₁ Then f₁ = p₁x+ q₁y + r₁*
Rule 2: *If x is A₂ and y is B₂ Then f₂ = p₂x + q₂y + r₂*
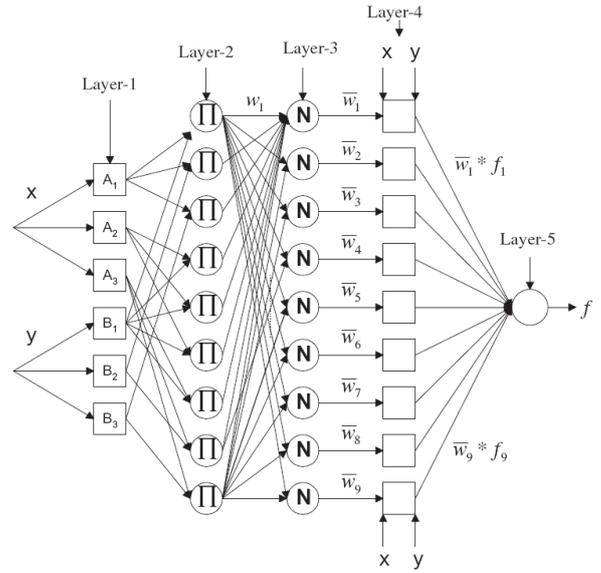
Fig. 3: Structure of ANFIS.

The general ANFIS control structure is presented here. This structure includes the same components as the fuzzy interference systems, except for the NN block. The structure of the network is comprised of a set of units (and connections) arranged into five connected network layers as shown in Figure 3, where square nodes are named adaptive nodes, to demonstrate that the parameters in these nodes are adjustable, while circle nodes are named fixed nodes, to demonstrate that the Parameters are fixed. Then the node function in each layer is described below:

Layer 1 (Fuzzy layer): This layer consists of membership functions of input variables. Every node *i* in this layer has a node function (Jang 1993[7]):

$$O_i^1 = \mu_{Ai}(x), O_i^1 = \mu_{Bi}(y), for\ i = 1,2,3 \qquad (6)$$

where *x* and *y* are inputs to node *i*, and O_i^1 is the membership function of *Ai* and *Bi* (linguistic labels for inputs).

Layer 2 (Production layer): Every node in this layer multiplies the incoming signals and sends the product out (Jang 1993[7]).

$$O_i^2 = w_i = \mu_{Ai}(x).\mu_{Bi}(y), for\ i = 1,2,3 \qquad (7)$$

Layer 3 (Normalized layer): The *i*th node of this layer calculates the ratio of the *i*th rules firing strength to the sum of all rules' firing strengths (Jang 1993[7]):

$$O_i^3 = \overline{w}_i = \frac{w_i}{w_1 + w_2 + \cdots + w_9}, for\ i = 1,2,\dots,9 \qquad (8)$$

Layer 4 (Defuzzy layer): Every node i in this layer has a node function (Jang 1993[7]):

$$O_i^4 = \overline{w}_i . f_i = \overline{w}_i . (p_i x + q_i y + r_i) \tag{9}$$

where w_i is the output of layer 3 and $\{p_i, q_i, r_i\}$ is the parameter set. Parameters in this layer will be referred to as consequent parameters.

Layer 5 (overall output layer): This layer sums up all the inputs coming from layer 4 and transforms the fuzzy classification results into a crisp (Jang 1993[7]).

$$O_i^5 = \sum_i \overline{w}_i f_i = \frac{\sum_i w_i f_i}{\sum_i w_i} \tag{10}$$

The ANFIS structure is adjusted automatically by least-square estimation & the back propagation algorithm. Because of its flexibility, the ANFIS strategy can be used for a wide range of control applications (Kusagur *et al.* 2010[13]).

5. ANFIS Inverse Training

The structure of the ANFIS inverse based control system is mainly composed of the ANFIS inverse network of the plant, which is used as a controller to generate the control action. To obtain the ANFIS inverse model of a plant, it is placed in series with the plant as shown in Figure 4. For the training, the input-output data set is used to reflect input-output characteristics of the plant.
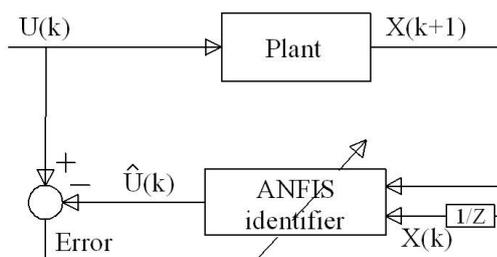

Fig. 4: The training process of ANFIS based on inverse plant model.

6. Proposed Control Strategy

6.1. ANFIS inverse controller

In this study, ANFIS based inverse model control is developed for semi-active control of structure. To do so, first an inverse emulator ANFIS of structure is trained. As shown in Figure 5, the input to this emulator is the structure's response, and the output is the actuator signal. The training

data is generated by actuating the structure and recording the sensor readings. When the trained inverse emulator is used as the controller, its input is the response of the structure under external excitation, and the ANFIS's output is the actuator signal required to reduce the response.
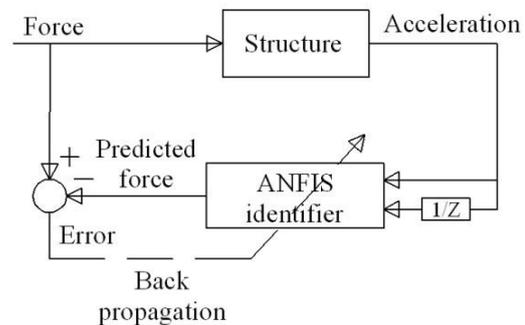

Fig. 5: The training process of inverse ANFIS of structure used in this study.

Effectiveness of the proposed controller is dependent on defining a correlation between response of structure and control signals. Here, ANFIS calculates control force based on current and previous time steps of acceleration feedback. Acceleration is selected for feedback control because accelerometers are durable measuring devices with a small power requirement which are widely available and relatively inexpensive (Schurter & Roschke 2001[22]). Three controllers are used for first, second and third story of the 3-story, and a controller is used for 76-story building. To actuate the structure for generating data, control force is generated randomly using band limited white Gaussian noise. Acceleration due to this force is calculated considering nonlinear material behavior described by Ohtori *et al.* (2004)[17] and briefly presented in this paper for 3- story and linear behavior for 76-story building.

By performing trial and error, it is seen that ANFIS structure with five triangular MFs for each input (25 if-then rules) and a linear output MF show satisfactory performance. Because the exact determination of input MFs coordinate is extremely complicated, they are assumed similar for simplicity.

6.2. Inverse MR Damper

The MR damper model estimates damper forces in response to the inputs of the reactive velocity and the issued voltage as described by Equations 2 to 5. Since the damper velocity is the same as the velocity of the floor to which the damper is connected, the voltage signal is the only parameter that can be altered to control the damper behavior to generate the required control force. Since the ANFIS controller estimates the required control force, in this study, the inverse behavior of the MR damper is modeled to solve the force tracking task by MR damper in the closed-loop cycle. To do so, a feed-forward back-propagation neural network is

constructed to copy the inverse dynamics of the MR damper (Fig. 6). To generate training data, the velocity and voltage are produced randomly using band limited white Gaussian noise and resulted force of the MR damper is calculated using the Equations 2 to 5. The sampling rate of the training data was 50 Hz for 90 sec periods, which resulted in 4500 patterns for training, testing and validation. The input states at time instant k for inverse model of MR damper are the damper velocity $\dot{x}(k)$ and desired control force $f_{des}(k)$ and the three previous histories of them, and the output state is current $v(k)$ (Fig. 6).

To select the network architecture, it is required to determine the transfer function, numbers of inputs, outputs, hidden layers, and nodes in the hidden layers, which are usually performed by trial and error. The most suitable input data in our case were found to be the current and the three previous histories for the damper velocity and desired control force. In addition, one hidden layer, with ten nodes, was adopted as one of the best suitable topologies for the NN. The tansig activation function is used for the hidden layer and the linear function for the output layer, which represents the control voltage.

Figure 7 shows the proposed control strategy which includes ANFIS controller, inverse NN model of MR damper and MR damper.
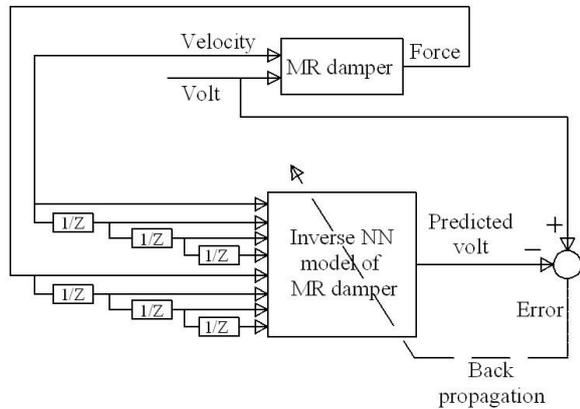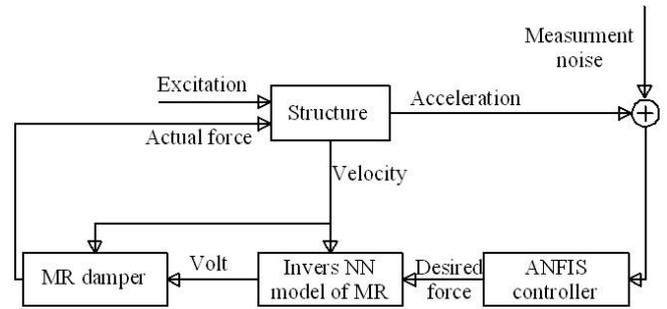

Fig. 7: Proposed control strategy.

7. Control Performance

To demonstrate the effectiveness of the proposed strategy, response of the 3-, and 76-story benchmark buildings excited by various earthquake records and wind are simulated, respectively. To verify the accuracy of the solver, the frequency and response of uncontrolled structures were compared with the benchmark problem papers (references [17] and [24])

The performance of the NN inverse model of MR damper is checked based on the comparison of the ideal force to the force generated by combining of the inverse MR damper and MR damper. Figure 8 shows the force generated by the MR damper compared with the ideal force generated randomly. It can be seen that the damper forces follow the target force closely. Figures 9 and 10 show the command voltage and the control force for 3-story and 76-story benchmark buildings, respectively.

Fig. 6: The training process of inverse model of MR damper.
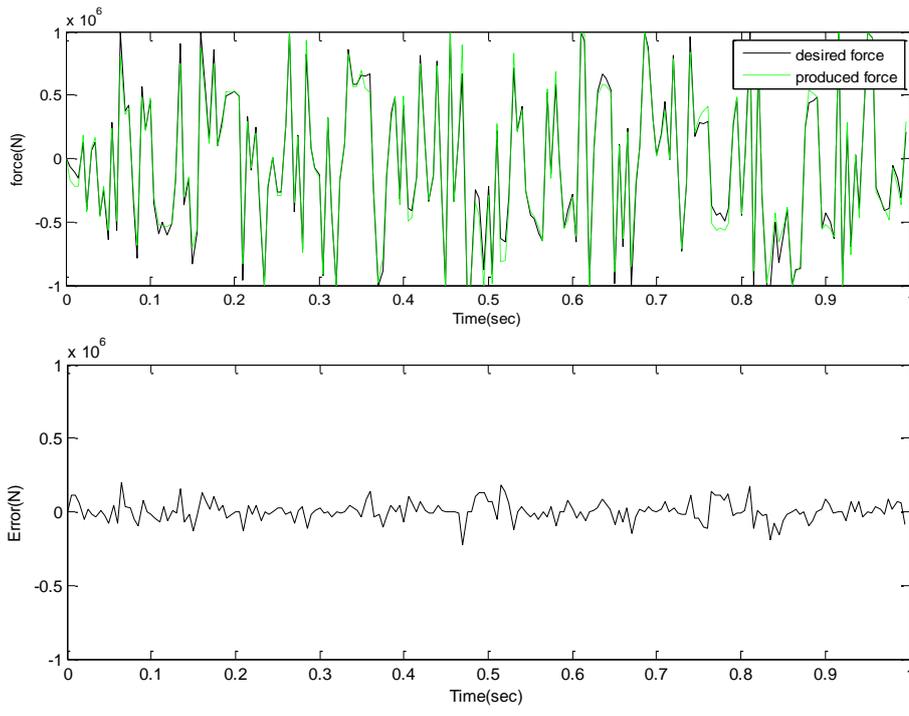
Fig. 8: Comparing desired force and produced force of MR damper.
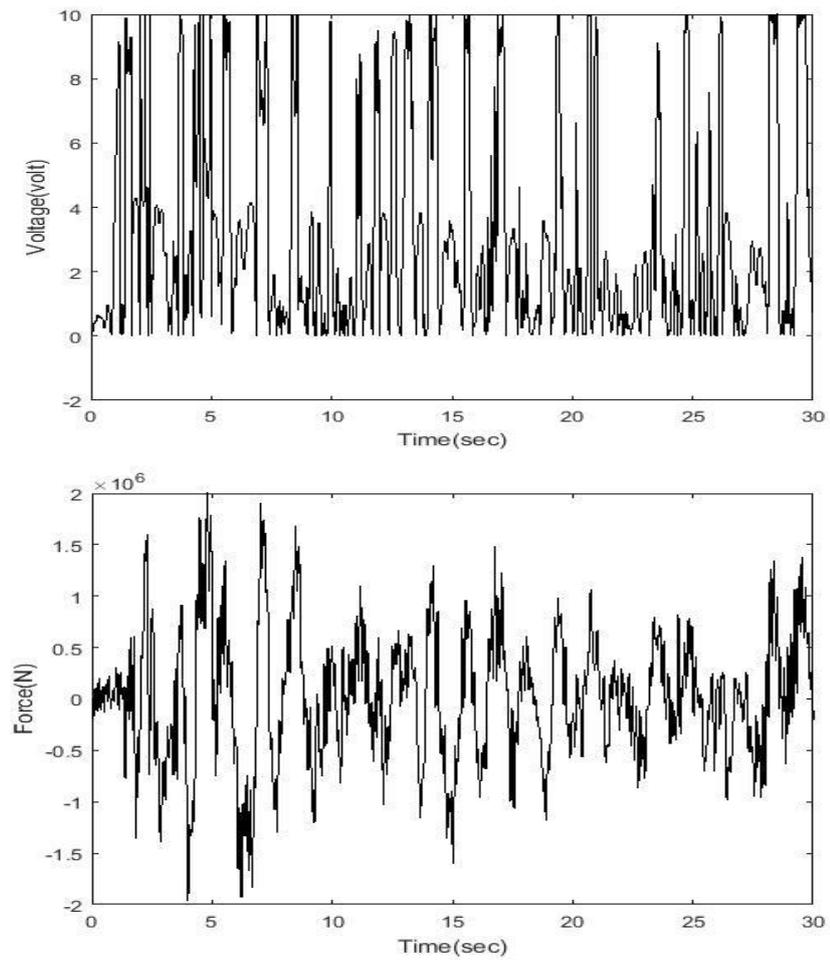
Fig. 9: Comand voltage and control force of story 2 for the 3-story benchmark building under the El Centro earthquake.
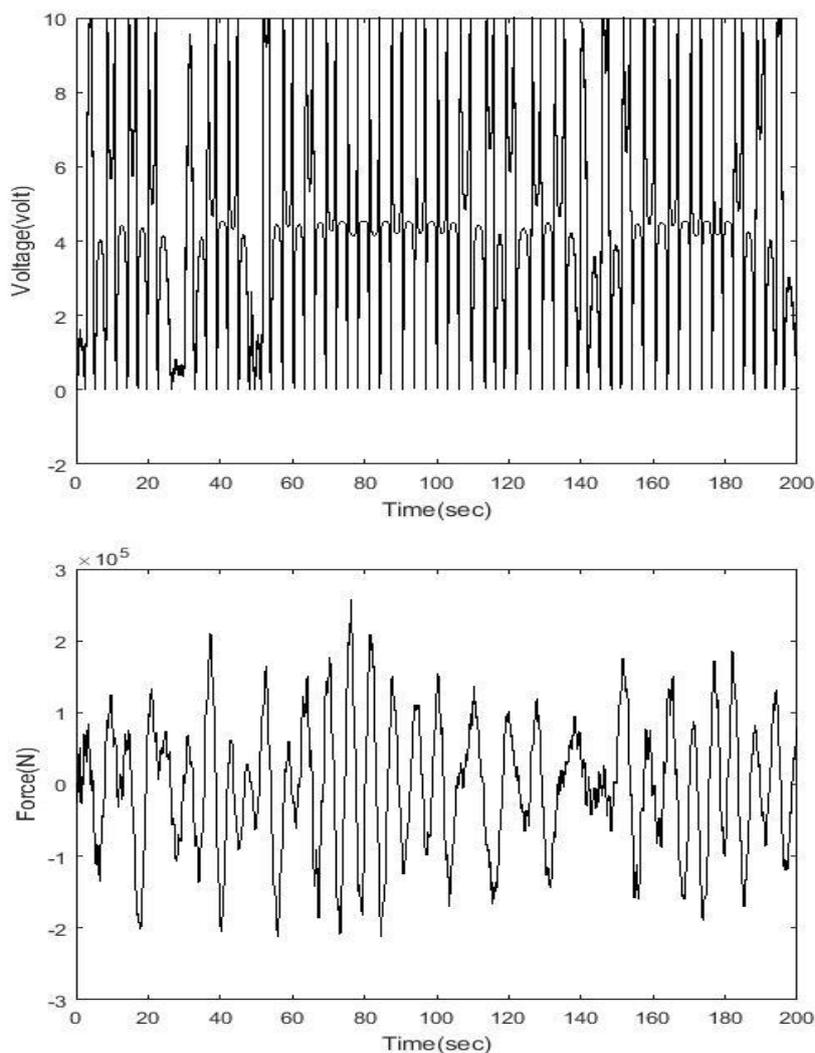
Fig. 10: Comand voltage and control force for the 76-story benchmark building.

7.1. 3-story building

To evaluate proposed control strategy, four historical records (two far-field and two near-field) are chosen as specified by Ohtori *et al.* (2004)[17] for the nonlinear benchmark buildings as follows: (1) *El Centro*. The N-S component recorded at the Imperial Valley Irrigation District substation in El Centro, California, during the Imperial Valley, California earthquake of May 18, 1940. (2) *Hachinohe*. The N-S component recorded at Hachinohe City during the Tokachi-oki earthquake of May 16, 1968. (3) *Northridge*. The N-S component recorded at Sylmar County Hospital parking lot in Sylmar, California, during the Northridge, California earthquake of January 17, 1994. (4) *Kobe*. The N-S component recorded at the Kobe Japanese Meteorological Agency station during the Hyogo-ken Nanbu earthquake of January 17, 1995. The absolute peak ground accelerations of these records are 3.417, 2.250, 8.2676, and 8.1782 m/sec^2, respectively. Totally, 10

earthquake records are considered in the evaluation of the control strategy, including: 0.5, 1.0 and 1.5 times the magnitude of El Centro and Hachinohe; and 0.5 and 1.0 times the magnitude of Northridge and Kobe.

To display the performance of the proposed controller, the relative displacement in the first story is compared in Figure 11 with the uncontrolled structure under the different earthquakes. As can be seen, the relative displacement is considerably reduced after control action. Additionally, it seems that the control algorithm can prevent the plastic deformations in Elcentro and Hachinohe earthquakes. However, because Northridge and Kobe earthquakes are near-field earthquakes, and they have a big PGA, the proposed controller could not prevent the plastic deformations.
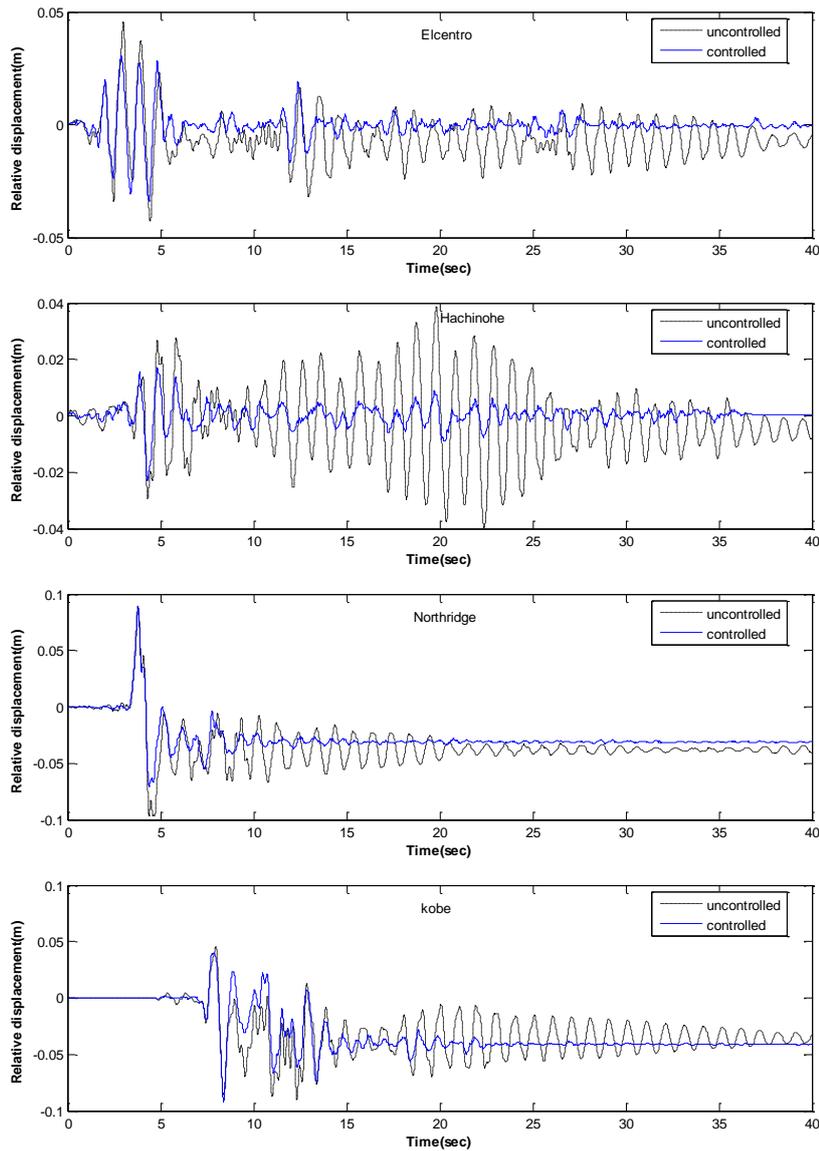
Fig. 11: Comparison of the first relative displacement for uncontrolled and ANFIS.

In addition, the performance of the controller is checked based on the evaluation criteria specified (J_1-J_6) for the nonlinear benchmark buildings (Ohtori *et al.* (2004)[17]), which are briefly presented in Table 2. These criteria are calculated as a ratio of the controlled and the uncontrolled responses. The first three criteria are established on peak interstory drift ratio (J_1), level acceleration (J_2) and base shear (J_3), over the range i=[1,3] where $d_i(t)$ is the interstory drift of story i over the time history of each earthquake, h_i is the height of story i, δ^{max} is the maximum interstory drift ratio of the uncontrolled structure computed using equation of $\max_{t,i}|d_i(t)/h_i|$, $\ddot{x}_{ai}(t)$ and $\ddot{x}_a^{max}$ are absolute acceleration of story i with and without control devices respectively, m_i is the seismic mass of story i and F_b^{max} is the maximum base shear of the uncontrolled structure for each respective earthquake.

The second three criteria are established on the building responses' norm. The inter story drift (J_4), level acceleration (J_5), and base shear (J_6) are defined by their norms, which are based on the structural forms. It should be added that the norm, $\|\,.\,\|$, is calculated by the following equation

$$\|\,.\,\| = \sqrt{\frac{1}{t_f}\int_0^{t_f}[\,.\,]^2 dt} \qquad (11)$$

and t_f is an adequately large time to allow the response of the structure to diminish.

To make a comparison, an active fuzzy controller called SOFLC designed by Al-Dawod *et al.* (2004)[1] and an active LQG controller are used. Moreover, two passive systems, passive off (POFF) and passive on (PON) are simulated. In these systems, voltage of MR dampers is set to minimum (zero) and maximum (ten) during the excitation, respectively.

Table 3 presents the evaluation criteria as the ratio of the controlled response to the uncontrolled response for each earthquake record individually for proposed controller (ANFIS), LQG, SOFLC, passive on and passive off control systems. This table shows that the proposed control system reduced J_1, J_2, J_3, J_4, J_5 and J_6, 33%, 9%, 3%, 29%, 38%, and 41%, respectively. In other words, ANFIS has a significant effect on normed interstory drift, acceleration and base shear and also peak of interstory drift, but a poor effect on peak acceleration and base shear. Comparing ANFIS and LQG controllers shows that the LQG performed slightly better than ANFIS controller.

Results also show that the passive on the system performed better than other systems in most criteria, especially the criteria associated to drift. This system decreased J_1 and J_4, 53% and 75% and also decreased J_2, J_3 and J_6, 16%, 13%, and 25%, respectively. Unfortunately, the normed acceleration is increased 80% using passive on the system; therefore, this system can't be used where occupant comfort is a high priority.

Table 3 also shows that passive off and SOFLC were by far the worst control systems, especially SOFLC that increased peak base shear, normed acceleration and normed base shear, 14%, 8%, and 27%, respectively.

7.2. 76-story building

In addition to simulation of the 3-story building under earthquake excitations, here, the 76-story benchmark building equipped with MR and TMD dampers is simulated under 500 seconds wind excitation to evaluate the proposed control strategy. The wind velocity can be separated into an average wind velocity and a wind fluctuation component. Consequently, the wind load composed of a static load due to the average wind velocity and a dynamic load due to wind velocity fluctuations. For structural control, only the fluctuating wind loads will be considered. Since the building is symmetric in both horizontal directions, the axis of elastic centers and the axis of mass centers coincide; therefore, there is no coupled lateral-torsional motion. Further, to reduce the computational efforts, only the along-wind motion will be considered. The Davenport wind load spectrum, which has been used in the Canadian design code, is used herein for along-wind loads.

The performance of the controller is evaluated based on the correlation of the response of controlled and uncontrolled building. Moreover, active LQG controller and passive TMD (PTMD) are used for comparison. Responses which are checked herein are the peak and RMS of displacement and acceleration for stories 1, 30, 50, 55, 60, 65, 70, 75 and 76.

Table 4 presents the results for different controllers and different stories. This table shows that the proposed controller (ANFIS) reduced the peak and RMS displacement of stories about 30% and 38%, respectively. In addition, the peak and RMS acceleration of stories are decreased about 50%.

Comparing the result for ANFIS and PTMD shows that although ANFIS didn't decrease the peak acceleration as much as PTMD, it decreased the peak and RMS displacement and RMS acceleration more than PTMD in deferent stories. Table 4 also shows that the active LQG controller reduced displacement and acceleration more than the proposed controller.

Table 2: Performance criteria for 3- story building.

$J_1 = average \; \underset{\substack{El \, Centro \\ Hachinohe \\ Northridge \\ Kobe}}{} \left\{ \dfrac{max_{t,i} \dfrac{\|d_i(t)\|}{h_i}}{\delta^{max}} \right\}$ Interstory drift ratio	$J_2 = average \; \underset{\substack{El \, Centro \\ Hachinohe \\ Northridge \\ Kobe}}{} \left\{ \dfrac{max_{t,i}\|\ddot{x}_{ai}(t)\|}{\ddot{x}_a^{max}} \right\}$ Level acceleration	$J_3 = average \; \underset{\substack{El \, Centro \\ Hachinohe \\ Northridge \\ Kobe}}{} \left\{ \dfrac{max_t\|\sum_i m_i \ddot{x}_{ai}(t)\|}{F_b^{max}} \right\}$ Base shear
$J_4 = average \; \underset{\substack{El \, Centro \\ Hachinohe \\ Northridge \\ Kobe}}{} \left\{ \dfrac{max_i \dfrac{\|d_i(t)\|}{h_i}}{\|\delta^{max}\|} \right\}$ Normed interstory drift ratio	$J_5 = average \; \underset{\substack{El \, Centro \\ Hachinohe \\ Northridge \\ Kobe}}{} \left\{ \dfrac{max_i\|\ddot{x}_{ai}(t)\|}{\|\ddot{x}_a^{max}\|} \right\}$ Normed level acceleration	$J_6 = average \; \underset{\substack{El \, Centro \\ Hachinohe \\ Northridge \\ Kobe}}{} \left\{ \dfrac{\|\sum_i m_i \ddot{x}_{ai}(t)\|}{\|F_b^{max}\|} \right\}$ Normed base shear

Table 3: Performance criteria for different controllers (3-story building).

Earthquake intensity) (	El centro (0.5)	El centro (1)	El centro (1.5)	Hachinohe (0.5)	Hachinohe (1)	Hachinohe (1.5)	Northridge (0.5)	Northridge (1)	Kobe (0.5)	Kobe (1)	average
J1 ANFIS	0.390	0.727	0.828	0.304	0.572	0.669	0.585	0.919	1.052	0.664	0.671
LQG	0.476	0.675	0.794	0.635	0.798	0.813	0.732	1.145	0.836	0.655	0.756
SOFLC	0.805	0.916	0.996	0.648	0.736	0.813	0.600	0.969	1.050	0.724	0.826
PON	0.270	0.479	0.711	0.155	0.221	0.357	0.391	0.750	0.752	0.608	0.470
POFF	0.938	0.961	0.983	0.782	0.986	0.969	0.988	1.027	0.993	0.901	0.953
J2 ANFIS	0.953	0.896	1.030	0.725	0.766	0.929	0.923	1.086	0.899	0.850	0.906
LQG	0.644	0.864	1.015	0.696	0.875	0.938	1.074	1.197	0.932	0.976	0.921
SOFLC	1.096	1.020	1.033	0.841	0.868	1.115	0.938	1.029	0.924	0.825	0.969
PON	0.652	0.910	1.193	0.721	0.456	0.745	0.818	1.034	1.111	0.790	0.843
POFF	0.966	0.991	1.000	0.886	1.002	0.990	1.008	0.993	0.930	0.980	0.975
J3 ANFIS	0.621	1.133	1.138	0.668	0.900	1.073	0.993	1.044	1.081	1.014	0.967
LQG	0.490	0.912	0.944	0.586	0.861	1.027	0.946	1.029	0.922	1.047	0.876
SOFLC	1.123	1.273	1.260	0.867	1.150	1.178	1.090	1.149	1.170	1.178	1.144
PON	0.617	0.921	1.113	0.522	0.635	0.864	0.744	1.043	1.145	1.076	0.868
POFF	0.980	1.023	0.995	0.806	1.000	0.980	1.004	1.002	0.977	0.999	0.977
J4 ANFIS	0.389	0.519	0.566	0.165	0.249	0.571	0.222	0.811	1.556	0.839	0.589
LQG	0.485	0.477	0.433	0.342	0.392	0.979	0.286	0.530	0.602	0.244	0.477
SOFLC	1.167	0.979	0.702	0.728	0.755	0.758	0.300	1.145	0.892	0.613	0.804
PON	0.184	0.228	0.256	0.118	0.111	0.139	0.071	0.752	0.547	0.122	0.253
POFF	0.897	0.824	1.022	0.807	0.958	1.227	0.975	1.026	0.685	0.752	0.917
J5 ANFIS	0.974	0.835	0.737	0.601	0.590	0.597	0.762	0.751	0.594	0.675	0.712
LQG	0.524	0.644	0.650	0.365	0.456	0.537	0.712	0.743	0.619	0.721	0.597
SOFLC	1.368	1.248	1.086	0.890	0.973	0.979	1.183	1.120	0.974	0.973	1.079
PON	2.894	1.703	1.250	2.210	1.285	1.046	2.411	1.655	1.965	1.574	1.799
POFF	0.905	0.901	0.909	0.816	0.949	0.960	0.926	0.931	0.891	0.947	0.914
ANFIS	0.613	0.782	0.737	0.342	0.408	0.503	0.739	0.740	0.634	0.735	0.623

J 6	LQG	0.489	0.606	0.608	0.351	0.439	0.522	0.671	0.668	0.560	0.675	0.559
	SOFLC	1.630	1.460	1.242	1.049	1.112	1.108	1.504	1.204	1.187	1.234	1.273
	PON	0.920	0.797	0.758	0.641	0.527	0.522	0.915	0.808	0.773	0.869	0.753
	POFF	0.905	0.896	0.906	0.818	0.954	0.966	0.941	0.931	0.885	0.942	0.914

Table 4: Performance criteria for different controllers (76-story building).

Criteria	Floor / Controller	1	30	50	55	60	65	70	75	76
Peak Displacement, cm (Percentage of Reduction)	ANFIS	0.04(27.4)	4.94(27.8)	11.83(28.6)	13.80(28.9)	15.82(29.2)	17.90(29.4)	19.99(29.6)	22.16(29.8)	22.65(29.9)
	LQG	0.03(37.2)	4.27(37.6)	10.20(38.5)	11.89(38.7)	13.63(39.0)	15.40(39.2)	17.20(39.5)	19.06(39.7)	19.48(39.7)
	PTMD	0.04 (25.8)	5.05(26.1)	12.10(27.0)	14.11(27.30)	16.18(27.5)	18.31(27.8)	20.45(28.0)	22.68(28.2)	23.18(28.2)
Peak Acceleration, cm/s^2(Percentage of Reduction)	ANFIS	0.38(-76.7)	4.19(41.3)	7.74(48.3)	9.09(48.0)	10.24(48.7)	11.49(49.1)	12.48(52.1)	14.02(53.8)	15.83(49.2)
	LQG	0.23(-6.7)	3.25(54.5)	6.50(56.5)	7.70(55.9)	8.93(55.2)	10.06(55.4)	10.62(59.2)	11.54(62.0)	15.86(49.1)
	PTMD	0.21(2.9)	3.80(46.9)	7.72(48.3)	8.84(49.4)	9.90(50.4)	11.3(49.8)	13.00(50.1)	15.12(50.1)	15.25(51.1)
RMS Displacement, cm (Percentage of Reduction)	ANFIS	0.010(37.8)	1.33(38.1)	3.22(38.4)	3.76(38.4)	4.32(38.5)	4.89(38.6)	5.47(38.7)	6.07(38.8)	6.21(38.8)
	LQG	0.01(42.0)	1.24(42.2)	3.00(42.5)	3.50(42.62)	4.02(42.7)	4.56(42.8)	5.10(42.9)	5.66(42.9)	5.78(42.9)
	PTMD	0.01(33.6)	1.43(33.8)	3.44(33.9)	4.03(34.0)	4.63(34.1)	5.25(34.1)	5.87(34.2)	6.52(34.2)	6.66(34.2)
RMS Acceleration, cm/s^2 (Percentage of Reduction)	ANFIS	0.06(-6.6)	1.10(45.7)	2.40(49.8)	2.81(49.8)	3.20(50.1)	3.63(50.3)	4.02(50.9)	4.44(51.4)	5.00(46.5)
	LQG	0.06(3.4)	0.90(55.7)	2.03(57.5)	2.41(56.9)	2.79(56.5)	3.14(57.0)	3.36(58.9)	3.35(63.4)	4.66(50.1)
	PTMD	0.06(2.9)	1.19(41.2)	2.68(44.00)	3.12(44.19)	3.55(44.6)	4.05(44.58)	4.54(44.5)	5.14(43.7)	5.23(44.1)

8. Conclusions

In this paper, ANFIS based inverse model control was developed for semi-active control of structure based on acceleration feedback. Unlike other methods, this approach didn't require other controllers to generate training data. MR dampers were used to provide control forces as semi-active devices. To set the command voltage of each damper in order to provide the desired force determined by ANFIS controller, an NN inverse model of the damper was designed. The effectiveness of proposed strategy was verified and illustrated using simulated response of a 3-story full-scale nonlinear benchmark building excited by various earthquake records, and a 76-story full-scale linear benchmark building excited by the 500 seconds Davenport wind load spectrum. To establish a context for evaluation effectiveness of the semi-active control scheme, responses to earthquake excitation for 3-story building, were compared with two active (LQG and SOFLC) and two passive (passive on and passive off) strategies. Moreover, the responses of the 76-story building were compared with the active LQG and passive TMD (PTMD).

Table 3 which presented the evaluation criteria as the ratio of the controlled response to the uncontrolled response for 3-story building showed that the proposed control system, ANFIS, significantly reduced normed drift, acceleration and base shear and also peak of inter story drift, and slightly reduced the peak acceleration and base shear. Results also showed that the passive on the system performed better than other systems in most criteria, except for normed acceleration. Both Passive off and SOFLC schemes were poor control systems, especially SOFLC that increased normed acceleration and base shear, and peak base shear. ANFIS and LQG controllers were between the best (passive on) and the worst (passive off and SOFLC) controllers. Figure 8 showed that the inverse NN model of MR damper could estimate the control voltage very well to produce the desired force. Results for 76-story building, which were presented in Table 4, showed that the active LQG controller reduced responses more than semi-active ANFIS, and semi-active ANFIS controller reduced them more than PTMD.

References

[1] Al-Dawod, M., Samali, B., Kwok, K. C. S., Naghdy, F., "Fuzzy controller for seismically excited nonlinear buildings", Journal of Engineering Mechanics, vol. 130(4), 2004, p. 407-415.

[2] Bani-Hani, K. A., Mashal, A., Sheban, M. A., "Semi-active neuro-control for base-isolation system using magnetorheological (MR) dampers", Earthquake Engineering & Structural Dynamics, vol. 35, 2006, p. 1119–1144.

[3] Choi, K. M., Cho, S. W., Jung, H. J., Lee, I. W., "Semi-active fuzzy control for seismic response reduction using magnetorheological dampers", Earthquake Engng Struct. Dyn., vol. 33, 2004, p. 723–736.

[4] Dyke, S. J., Spencer, B. F., Sain, M. K., Carlson, J. D., "Modeling and control of magnetorheological dampers for seismic response reduction", Smart Materials and Structures, vol. 5, 1996, p. 565–575.

[5] Dyke, S. J., Yi, F., Carlson, J. D., "Application of magnetorheological dampers to seismically excited structures", Proc., Int. Modal Anal. Conf., Bethel, Conn, 1999.

[6] Gu, Z. Q., Oyadiji, S. O., "Application of MR damper in structural control using ANFIS method", Computers and Structures, vol. 86, 2008, p. 427–436.

[7] Jang, J. S. R., "ANFIS: Adaptive network-based fuzzy inference systems", IEEE Transactions on Systems, Man, and Cybernetics, vol. 23, 1993, p. 665–685.

[8] Jung, H. J., Lee, H. J., Yoon, W. H., Oh, J. W., Lee, I. W., "Semiactive neurocontrol for seismic response reduction using smart damping strategy", Journal of Computing in Civil Engineering, vol. 18(3), 2004, p. 277–280.

[9] Kadhim, H. H., "Self Learning of ANFIS Inverse Control using Iterative Learning Technique", International Journal of Computer Applications, vol. 21(8), 2011, p. 24-29.

[10] Karamodin, A., Irani, F., Baghban, A., "Effectiveness of a fuzzy controller on the damage index of nonlinear benchmark buildings", Scientia iranica A, vol. 19(1), 2012, p. 1-10.

[11] Kerboua, M., Benguediab, M., Megnounif, A., Benrahou, K. H., Kaoulala, F., "Semi active control of civil structures, analytical and numerical studies", Physics Procedia, vol. 55, 2014, p. 301-306.

[12] Kumar, R., Singh, S. P., Chandrawat, H. N., "MIMO adaptive vibration control of smart structures with quickly varying parameters: Neural networks vs classical control approach", Journal of Sound and Vibration, vol. 307, 2007, p. 639–661.

[13] Kusagur, A., Kodad, S. F., Ram, B. V. S., "Modeling, Design & Simulation of an Adaptive Neuro-Fuzzy Inference System (ANFIS) for Speed Control of Induction Motor", International Journal of Computer Applications, vol. 6(12), 2010, p. 29-44.

[14] K-Karamodin, A., H-Kazemi, H., Akbarzadeh-T, M. R., "Semi-active control of structures using neuropredictive algorithm for MR dampers", 14th World Conference on Earthquake Engineering, Beijing, China, 2008.

[15] Lee, H. J., Yang, Y. G., Jung, H. J., Spencer, B. F., Lee, I. W., "Semi-active neurocontrol of a base isolated benchmark structure", Structural Control and Health Monitoring, vol. 13, 2006, p. 682–692.

[16] Marinaki, M., Marinakis, Y., Stavroulakis, G. E., "Fuzzy control optimized by a multi-objective differential evolution algorithm for vibration suppression of smart structures", Computers & Structures, vol. 147, 2015, p. 126-137.

[17] Ohtori, Y., Christenson, R. E., Spencer, Jr. B. F., Dyke, S. J., "Benchmark control problems for seismically excited nonlinear buildings", Journal of Engineering Mechanics, vol. 130(4), 2004, p. 366–387.

[18] Ohtori, Y., Spencer, B.F. Jr., "A MATLAB-based tool for nonlinear structural analysis", In the proceeding of the 13th ASCE engineering mechanics division specialty conference, Johns Hopkins university, Baltimore, June13-16, 1999.

[19] Park, K-S., Ok, S-Y., "Modal-space reference-model-tracking fuzzy control of earthquake excited structures", Journal of Sound and Vibration, vol. 334, 2015, p. 136-150.

[20] Pourzeynali, S., Lavasani, H. H., Modarayi, A. H., "Active control of high rise building structures using fuzzy logic and genetic Algorithms", Engineering Structures, vol. 29, 2007, p. 346-357.

[21] Rezaiee-Pajand, M., Akbarzadeh-T., M. R., Nikdel, A., "Direct adaptive neurocontrol of structures under earth vibration", Journal of Computing in Civil Engineering, vol. 23(5), 2009, p. 299-307.

[22] Schurter, K. C., Roschke, P. N., "Neuro-Fuzzy Control of Structures Using Magnetorheological Dampers", Proceedings of the American Control Conference, Arlington, 2001, p. 25-27.

[23] Xu, Y. L., Qu, W. L., Ko, J. M., "Seismic response control of frame structures using magnetorheological/ electrorheological dampers", Earthq. Eng. Struct. Dyn., vol. 29, 2000, p. 557–75.

[24] Yang, J., Wu, J., Samali, B., Agrawal, A., "A benchmark problem for response control of wind-excited tall building", Web Site (http://www.eng.uci.edu/~jnyang/benchmark.htm), 1999.

[25] Yi, F., Dyke, S. J., Caicedo, J. M., Carlson J. D., "Experimental Verification of Multi-Input Seismic Control Strategies for Smart Dampers", Journal of Engineering Mechanics, vol. 127(11), 2001, p. 1152–1164.

[26] Yi, F., Dyke, S. J., Caicedo, J. M., Carlson, J. D., "Seismic Response Control Using Smart Dampers", Proc., American Control Conference, San Diego, CA, 2009, p. 1022–1026.